

Bridgman growth and magneto-optical properties of CeF₃ crystal as Faraday Rotator

Huifang Li^{a,b}, Jingya Wang^b, Junfeng Chen^b, Yun Dai^b, Liangbi Su^b, Xiang Li^{a,*}, A. M. Kalashnikova^c, Anhua Wu^{b,**}

^a School of Materials Science and Engineering, University of Shanghai for Science and Technology, Shanghai, 200093, China

^b Synthetic Single Crystal Research Center and Key Laboratory of Transparent and Opto-functional Inorganic Materials, Shanghai Institute of Ceramic, Chinese Academy of Sciences, Shanghai, 200050, China

^c Ioffe Institute, Russian Academy of Sciences, Politeknicheskaya 26, 194021, St. Petersburg, Russia

ARTICLE INFO

Keywords:

Crystal growth
Bridgman-Stockbarger method
Magneto-optical properties

ABSTRACT

In this work, CeF₃ crystal with maximum diameter of 35 mm was successfully grown with the Bridgman-Stockbarger (BS) method. The crystal diffraction peaks match well with the standard pattern of CeF₃ (PDF#01-089-0967), which proves that obtained samples are of high purity. The transmittance of CeF₃ crystal is relatively high in the UV-NIR region and reach 92% in comparison with TGG crystal. The UV cut-off absorption edge of CeF₃ crystal is located at 270 nm contrary to 400 nm for TGG. The Verdet constant of CeF₃ crystal is largest at 450 nm wavelength and reach 247 rad/T m. The results show that CeF₃ possess better optical and magneto-optical properties than TGG. CeF₃ can be a potential candidate for Faraday Rotators used in the field of high-power lasers.

1. Introduction

In recent years, diode pumped solid state lasers (DPSSL) play an important role in military, processing, medical and scientific research applications [1–3]. Faraday Rotators (FR) as a key component of DPSSL can protect laser devices and laser amplifiers from backlight [4–6]. A traditional FR material, TGG crystal gained much attention in commercial applications due to its high Verdet constant, especially in the visible wavelength region (>395 nm) [7,8]. However, there are several disadvantages of TGG crystal that restricts its further utilization. The examples are: complex synthesis process, high cost, increasing absorption losses in the visible (VIS) range and a possession of absorption edge at 400 nm. TGG can neither be used at wavelengths beneath 400 nm nor at around 490 nm. Therefore, it is urgent to find a material that can replace TGG in aforementioned wavelength ranges.

It is well known that among the rare earths, ions such as, Ce³⁺, Pr³⁺, Dy³⁺ and Tb³⁺ have been pointed to possess the excellent MO properties [9,10] due to their 4f-5d transitions [11]. Ce³⁺ is characterized by a full transparency in the VIS region compared to other mentioned RE³⁺ [12], and has the highest concentration among RE³⁺-fluorides [13]. A proven

production technology is a significant advantage of the CeF₃ crystal over other novel magnetically activated media, since this material has long been used in scintillation detectors [14,15]. Compared with the TGG crystal, the CeF₃ has similar Verdet constant, lower absorption coefficient and wider transmission wavelength range [16]. Due to aforementioned advantages, CeF₃ could substitute TGG in Faraday Rotators.

The theory of the Faraday effect has been distinguished and calculated by Serber, including the effects of the components of magnetic moment [17]. It was the first time shown by Faraday Rotation that optical activity in material is induced by a magnetic field and revealed the nature of magnetic optical properties especially in regions of absorption [18]. The Verdet constant of CeF₃ crystal in the 450–1550 nm had been also measured in the previous works [19], but not for Faraday Rotation angle. At the same time, the optical Faraday Rotation has been investigated in the temperature range 8–300 K at 632.8 nm wavelength [20–22], missing the data over 800 nm, whereas the majority of the available high-power lasers process in this range.

In this work, the Bridgman growth of CeF₃ crystal was investigated. The dependence of the Faraday Rotation angle on visible to near-infrared whole wavelengths were systematically studied by using

* Corresponding author.

** Corresponding author.

E-mail addresses: xiangli@usst.edu.cn (X. Li), wuanhua@mail.sic.ac.cn (A. Wu).

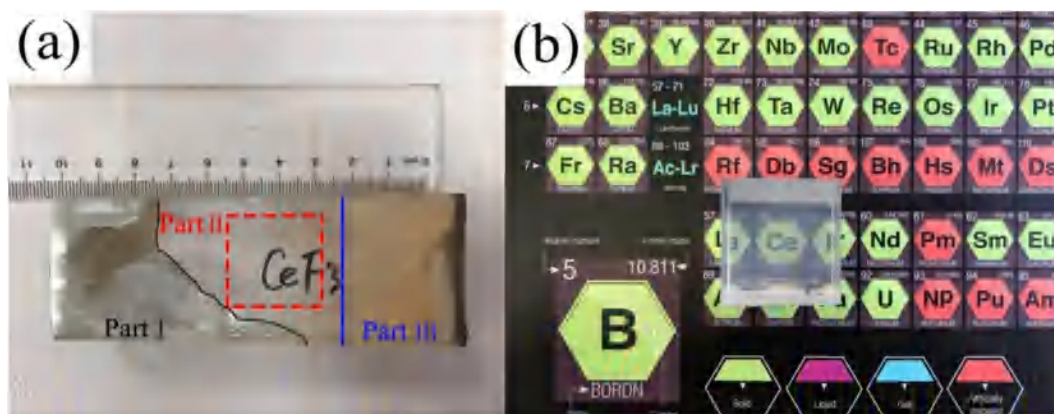


Fig. 1. Photographs of as-grown crystal and processed sample: (a) as-grown block CeF_3 crystal grown by the Vertical Bridgman method and (b) the (001)-oriented part II sample cut from the crystal ingot.

continuously changing magnetic field. Meanwhile, a huge potential for utilization of CeF_3 was predicted as a NIR high-power laser FR for a broad variety of wavelengths.

2. Experimental procedure

2.1. Processing of raw materials

The growth of high-quality CeF_3 crystal by the Bridgman method is reported using CeF_3 (99.999%) and PbF_2 (99.999%) powders as raw materials. Commercial CeF_3 raw material cannot be used directly for the growth due to the presence of moisture and oxides. To get rid of oxygen and water, CeF_3 raw material underwent an effective fluoridation treatment. At the same time, PbF_2 is used as an oxygen scavenger to eliminate residual oxygen during crystal growth. CeF_3 and PbF_2 powders were weighed on the basis of the certain proportion.

2.2. Preparation of precursor

A total of 400–500g of materials were charged in a columnar-shaped crucible, which was put into a quartz glass tube in a resistive heating furnace. A gaseous HF of high purity (4 N) was used as the gas source in the process. The starting materials were heated at 200–230 °C in dry HF gas flow for 6–7 h to eliminate the moisture absorbed. By this way, the moisture in the raw materials was thoroughly removed. As the fluoridation process was terminated, the HF gas flow was ceased and the furnace was cooled. Then the vacuum was used for driving away residual HF gas and the exhaust gas was absorbed by Na_2CO_3 solution.

2.3. Crystal growth

The feed materials for crystal growth were prepared of CeF_3 and PbF_2 powders. They were mixed and loaded into the graphite crucible located vertically in the furnace. To avoid the oxidation of the melt, the assembled crucible was sealed immediately. By means of sealing the graphite crucible firmly, it was possible to grow the fluoride crystal in a nonvacuum atmosphere. Whereas, in normal atmosphere, there was always a volume of air that remained in the crucible when it was sealed. When the growth process finished, the furnace was cooled down slowly to a room temperature and then as-grown crystal was moved to the annealing furnace.

2.4. Characterizations

The X-ray diffraction analysis of the grown crystal was performed with the Ultima IV (Rigaku, Japan). The powder diffraction measurements of CeF_3 grounded crystal as well as a-axis and c-axis samples were

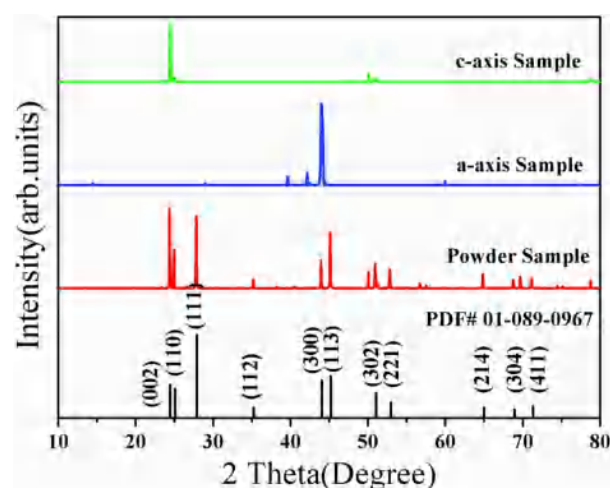


Fig. 2. XRD patterns of CeF_3 crystal powder, a-axis and c-axis samples as-grown by the Bridgman method compared with the standard card of CeF_3 numbered 01-089-0967.

done using Bruker D8 diffractometer with $\text{Cu K}\alpha$ radiation ($\lambda = 1.54056 \text{ \AA}$) at a scan step of 0.02° . The optical transmission spectra of the CeF_3 crystal part II and part III were measured by VARIAN CARY 5000 UV-VIS-NIR Spectrometer at room temperature. We measured the dependence of the Verdet constant on wavelength in the 450–1310 nm range using different wavelengths (450 nm, 532 nm, 633 nm, 810 nm, 980 nm, 1075 nm, 1310 nm) at room temperature. The Faraday Rotation angle in function of magnetic field strength was measured using homemade system provided by University of Electronic Science and Technology of China.

3. Results and discussion

As shown in Fig. 1(a), it is observed that the crystal consist three parts, the polycrystalline part I resulted from its weak bending force, the transparent part II and nontransparent part III caused by the oxygen impurities. According to the cleavage plane of cerium fluoride crystal perpendicular to the optical axis, the (001)-oriented sample with $20 \times 20 \times 20$ mm dimensions was cut out from the part II, and both sides were further polished as shown in Fig. 1 (b). Similarly, the (100)-oriented and (001)-oriented crystals can be obtained by the above processing.

The phases present in the ingot were analyzed using X-ray diffraction. The cuboid sample was collected from the part II of the ingot and

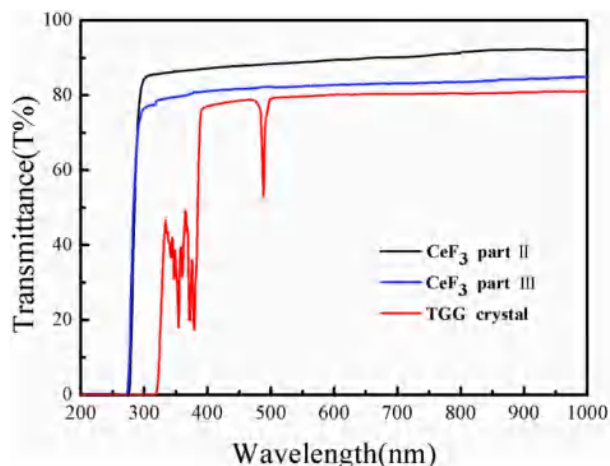


Fig. 3. Transmission spectra of CeF₃ crystals in different positions in comparison with the reference crystal TGG.

fine powders from grinding of the ingot. Fig. 2 shows the obtained XRD patterns. The lattice constants of the sample (from the part II) were determined to be $a = b = 7.112 \text{ \AA}$, $c = 7.279 \text{ \AA}$ using Jade software. XRD patterns of (100) and (001)-orientated samples match well with the standard pattern (PDF#01-089-0967), confirming the sample is a single-phase hexagonal system with a space group $P3(-)c1$ and six molecules per unit cell [23].

In order to evaluate the quality for different parts of the ingot and to compare the corresponding performance with TGG, the parts II and III (the two parts cut from CeF₃ ingot) and a TGG sample were selected for characterization. Fig. 3 shows the corresponding transmission spectra in the UV-NIR region. It can be observed that two CeF₃ samples are completely transparent in the UV-NIR region and possess short-wave absorption cut-off edges at 270 nm. The part II has a higher transmittance than part III for wavelengths higher than 336 nm. An average transmission, ranging between 86% and 92%, may be attributed to the presence of scattering centers in the bulk of the CeF₃ crystal and the quality of the surface polishing.

The average transmittance of the part III above 350 nm equals 80% without any absorption band. This may be caused by segregation of impurities during the growth process. Such segregation is the main reason of the transmittance gradient along different parts of the crystal. The impurities were gradually accumulated as crystallization front traversed the crucible during growth. This is the reason why the transmittance of part III is worse than part II. For TGG crystal, a strong

absorption peak related to (${}^7F_6 \rightarrow {}^5D_4$ transition of Tb³⁺ ions) can be observed at 488 nm, which severely restricts the application of TGG as FRs in the visible region. In this sense, CeF₃ is a good replacement for TGG in application as FR.

To evaluate the rotation efficiency of CeF₃ crystal, the magneto-optical properties of CeF₃ and TGG crystal were characterized. The crystal structures of CeF₃ and NdF₃ has been proved to be a hexagonal tisonite-type structure (space group $P-3c1$, $Z = 6$), whose third-order optical axis coincides with the crystallographic c -axis. All the investigations were performed for the samples cut perpendicular to the optical axis because only on this account the influence of the natural birefringence on the Faraday Rotation measurement results [10] can be excluded. Fig. 4a and b shows the magnetic field strength dependences of Faraday Rotation angle in the external magnetic field for the CeF₃ crystal oriented along c -axis and the TGG one, respectively. It can be observed that for a given wavelength, the plots of Faraday Rotation angle vs the magnetic field of both CeF₃ crystal and TGG crystals have a

Table 1

Magneto-optical properties of CeF₃ and TGG crystals.

λ (nm)	450	532	633	810	980	1075	1310
$V(\lambda)_{\text{CeF}_3}$, rad/T m	247	180	129	63	44	33	10
$V(\lambda)_{\text{TGG}}$, rad/T m	408	205	137	75	47	35	14

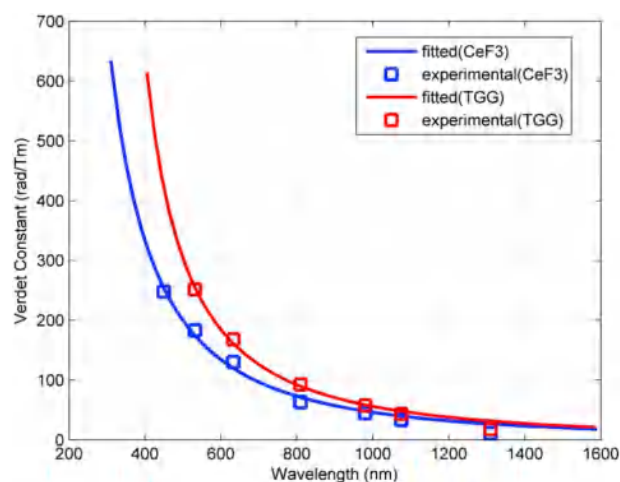


Fig. 5. Figure of Verdet Constant Dispersion as a function of the wavelength for CeF₃ in comparison with TGG.

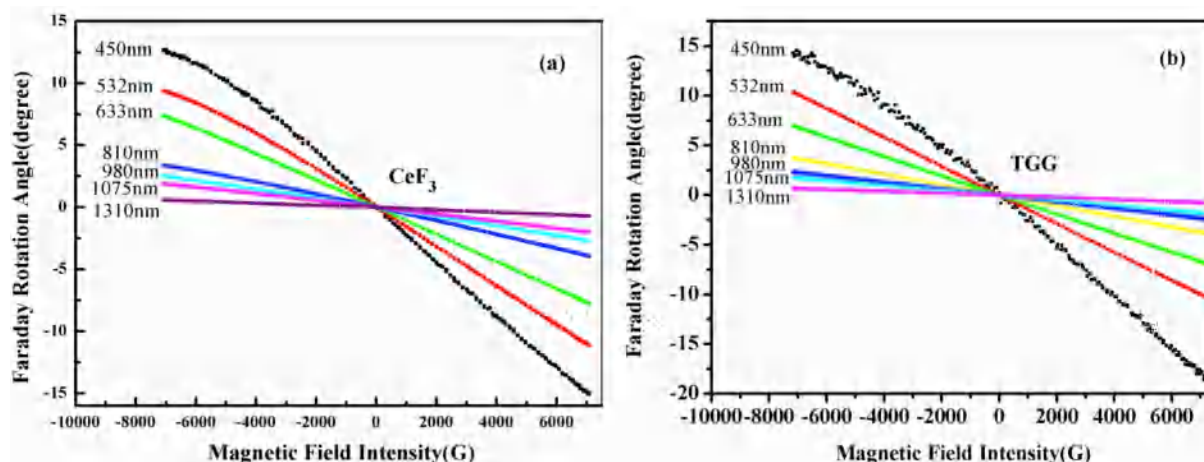


Fig. 4. Faraday Rotation angle as a function of the magnetic field strength for (a)CeF₃ and (b) TGG.

symmetry center with point (0, 0). The absolute values of Faraday Rotation angle increase with increase of magnetic field, according to the Faraday equation $\beta = VBL$, where V is Verdet constant, B represents the magnetic field strength and L stands for the crystal length. The slope of the fitted curve for both CeF_3 and TGG sample increase with decrease of a wavelength. (as shown in Table 1) This behavior is consistent with the previous data [13]. For CeF_3 Verdet constant value at 450 nm, equals 247 rad/T m. The value of TGG Verdet constant at 450 nm is 408 rad/T m.

The measured values are used to find the dependence of the Verdet constant of the CeF_3 crystal on the radiation wavelength. The Verdet constant fitting values as a function of wavelength are depicted in Fig. 5. In the approximation of the single-oscillator model of the permitted electronic $4f \rightarrow 5d$ transition in the Ce^{3+} ions, the spectral V dependence can be described by the spectral one of "paramagnetic" c-term of FR [24, 25].

$$V = C\omega^2 / \omega_0^2 - \omega^2 = A / \lambda^2 - \lambda_0^2$$

where λ_0 is relevant to the $4f \rightarrow 5d$ transition wavelength of the RE^{3+} ions, and the factor E is in direct proportion to the concentration of magnetic ions per volume, the Lande splitting factor, and the transition probability. The parameters A and λ_0 of CeF_3 and TGG crystals were found by the least squares method to be $A = 4.4 \times 10^7 \text{ rad} \cdot \text{nm}^2 / (\text{T} \cdot \text{m})$ and $\lambda_0 = 159 \text{ nm}$, $A = 5.1 \times 10^7 \text{ rad} \cdot \text{nm}^2 / (\text{T} \cdot \text{m})$ and $\lambda_0 = 283 \text{ nm}$, respectively.

4. Conclusions

The CeF_3 crystal was grown successfully by the Vertical Bridgman process. Commercial CeF_3 raw materials were treated in an electric resistive furnace to remove moisture and residual oxides. The CeF_3 single crystal exhibit transmittance as high as 92% without any absorption band compared to the traditional FR material TGG. In addition, the CeF_3 single crystal can complement the failing magneto-optical properties at 450 nm, and its Verdet constant can reach 247 rad/T m at 450 nm. The results show that CeF_3 crystal is a promising magneto-optical material in the VIS–NIR range. Further experiments are needed to prove its usability as the optical isolator for the strong laser field.

Declaration of competing interest

The authors declare that they have no known competing interests or personal relationships that could have appeared to influence the work reported in this paper.

CRediT authorship contribution statement

Huifang Li: Conceptualization, Methodology, Investigation, Data

curation, Writing - original draft, Writing - review & editing. **Jingya Wang:** Conceptualization, Methodology, Formal analysis. **Junfeng Chen:** Resources, Investigation. **Yun Dai:** Investigation. **Liangbi Su:** Supervision, Project administration. **Xiang Li:** Conceptualization, Writing - review & editing. **A.M. Kalashnikova:** Supervision. **Anhua Wu:** Conceptualization, Methodology, Supervision, Funding acquisition, Writing - review & editing, Project administration.

Acknowledgments

This work was supported by the National Natural Science Foundation of China (NSFC, Grants No. 51872309, U1832106) and the Science and Technology Commission of Shanghai Municipality (No.19520710900) This work was also supported by the funding of CAS International Cooperation Project (No.121631KYSB20180045) and CAS Special international exchange project.

Authors would like to thank Prof. Lei Bi from the University of Electronic Science and Technology of China for his kind help with experimental part.

References

- [1] M. Frank, S.N. Smetanin, M. Jelinek, *Opt. Laser. Technol.* 119 (2019) 105660.
- [2] Q. Shen, X.Y. Cui, M.C. Yan, *Opt. Express* 27 (2019) 31913.
- [3] E. Beyatli, *Opt. Commun.* 451 (2019) 55.
- [4] R. Yasuhara, A. Ikesue, *Opt. Express* 27 (2019) 7485.
- [5] A. Ikesue, Y.L. Aung, *J. Am. Ceram. Soc.* 101 (2018) 5120.
- [6] A. Ikesue, Y.L. Aung, S. Makikawa, *Opt. Lett.* 42 (2017) 4399.
- [7] W. Jin, J. Ding, L. Guo, *J. Cryst. Growth* 484 (2018) 17.
- [8] U. Valiev, J. Gruber, D. Sardar, *Opt Spectrosc.* 102 (2007) 910.
- [9] S. Berger, C. Rubinstein, C. Kurkjian, *Phys. Rev.* 133 (1964) A723.
- [10] J.F. Nye, *Physical Properties of Crystals*, Oxford University Press, 1964.
- [11] P. Dorenbos, *J. Lumin.* 91 (2000) 155.
- [12] E.G. Villora, K. Shimamura, G.R. Plaza, *J. Appl. Phys.* 117 (2015) 233101.
- [13] V. Vasylyev, E.G. Villora, M. Nakamura, *Opt. Express* 20 (2012) 14460.
- [14] C. Pedrini, A. Belsky, *Acta Physica Polonica-Series A General Physics* 84, 1993, p. 953.
- [15] P. Belli, R. Bernabei, R. Cerulli, et al., *Nucl. Instrum. Methods Phys. Res. Sect. A Accel. Spectrom. Detect. Assoc. Equip.* 498 (2003) 352.
- [16] P. Molina, V. Vasylyev, E. Villora, *Opt. Express* 19 (2011) 11786.
- [17] R. Serber, *Phys. Rev.* 41 (1932) 489.
- [18] A.D. Buckingham, P.J. Stephens, *Annual Review of Physical Chemistry* 17, 1966, p. 399.
- [19] E.A. Mironov, A.V. Starobor, *Opt. Mater.* 69 (2017) 196.
- [20] U.V. Valiev, D.N. Karimov, *J. Appl. Phys.* 121 (2017) 243105.
- [21] J. Picard, H. Le-Gall, C. Leycuras, *Comptes Rendus Hebd. Seances Acad. Sci. Ser. A B* 14 (1979) 221.
- [22] C. Leycuras, H. Le Gall, M. Guillot, *J. Appl. Phys.* 55 (1984) 2161.
- [23] N. Bolotina, T. Chernaya, I. Verin, *Crystallogr. Rep.* 61 (2016) 29.
- [24] G. Liu, W. Zhang, X. Zhang, *Phys. Rev. B* 48 (1993) 16091.
- [25] A.D. Buckingham, P.J. Stephens, *Annu. Rev. Phys. Chem.* 17 (1966) 399.